

Prepublished online May 21, 2012; doi:10.1182/blood-2011-11-394072

Eri1 regulates microRNA homeostasis and mouse lymphocyte development and anti-viral function

Molly F. Thomas, Sarah Abdul-Wajid, Marisella Panduro, Joshua E. Babiarz, Misha Rajaram, Prescott Woodruff, Lewis L. Lanier, Vigo Heissmeyer and K. Mark Ansel

Information about reproducing this article in parts or in its entirety may be found online at: http://bloodjournal.hematologylibrary.org/site/misc/rights.xhtml#repub_requests

Information about ordering reprints may be found online at: http://bloodjournal.hematologylibrary.org/site/misc/rights.xhtml#reprints

Information about subscriptions and ASH membership may be found online at: http://bloodjournal.hematologylibrary.org/site/subscriptions/index.xhtml

Advance online articles have been peer reviewed and accepted for publication but have not yet appeared in the paper journal (edited, typeset versions may be posted when available prior to final publication). Advance online articles are citable and establish publication priority; they are indexed by PubMed from initial publication. Citations to Advance online articles must include the digital object identifier (DOIs) and date of initial publication.



Eri1 regulates microRNA homeostasis and mouse lymphocyte development and anti-viral function

Molly F. Thomas^{1,2}, Sarah Abdul-Wajid^{1,2}, Marisella Panduro^{1,2}, Joshua E. Babiarz³, Misha Rajaram⁴, Prescott Woodruff^{4,5}, Lewis L. Lanier¹, Vigo Heissmeyer⁶, K. Mark Ansel^{1,2}

- $^{\rm 1}$ Department of Microbiology & Immunology, University of California San Francisco, San Francisco, CA 94143
- 2 Sandler Asthma Basic Research Center, University of California San Francisco, San Francisco, CA 94143
- ³ Eli and Edythe Broad Center of Regeneration Medicine and Stem Cell Research, Center for Reproductive Sciences, and Department of Urology, University of California San Francisco, San Francisco, CA 94143
- ⁴ Cardiovascular Research Institute, University of California San Francisco, San Francisco, CA 94143
- ⁵ Division of Pulmonary and Critical Care Medicine, Department of Medicine, University of California San Francisco, San Francisco, CA 94143
- ⁶ Helmholtz Zentrum München, German Research Center for Environmental Health, Institute of Molecular Immunology, 81377 Munich, Germany

Running title: Eri1 regulates microRNA homeostasis in lymphocytes

Corresponding Author: K. Mark Ansel, Ph.D. University of California San Francisco Department of Microbiology & Immunology 513 Parnassus Avenue, Box 0414 San Francisco, CA 94143-0414

Phone: 1 415 476 5368 Fax: 1 415 502 4995

Email: mark.ansel@ucsf.edu

ABSTRACT

Natural killer (NK) cells play a critical role in early host defense to infected and transformed cells. Here we show that mice deficient in Eri1, a conserved 3'-to-5' exoribonuclease that represses RNA interference, have a cell-intrinsic defect in NK cell development and maturation. *Eri1-/-* NK cells displayed delayed acquisition of Ly49 receptors in the bone marrow and a selective reduction in Ly49D and Ly49H activating receptors in the periphery. Eri1 was required for immune-mediated control of mouse cytomegalovirus (MCMV) infection. Ly49H* NK cells deficient in Eri1 failed to expand efficiently during MCMV infection, and virus-specific responses were also diminished among *Eri1-/-* T cells. We identified miRNAs as the major endogenous small RNA target of Eri1 in mouse lymphocytes. Both NK and T cells deficient in Eri1 displayed a global, sequence-independent increase in miRNA abundance. Ectopic Eri1 expression rescued defective miRNA expression in mature *Eri1-/-* T cells. Thus, mouse Eri1 regulates miRNA homeostasis in lymphocytes and is required for normal NK cell development and anti-viral immunity.

INTRODUCTION

Natural Killer (NK) cells are important lymphocyte effectors that participate in early immune responses against tumors and pathogen-infected cells by secreting cytokines and directly lysing target cells.¹ Unlike T and B cells, which become activated through single antigen-specific receptors, NK cell activation is controlled by the integration of signals from activating and inhibitory receptors.² The inhibitory mouse Ly49 receptors are a highly polymorphic class of molecules that predominantly recognize major histocompatibility complex (MHC) class I ligands. In contrast, Ly49 activating receptors can bind MHC class I molecules or ligands expressed on transformed or infected cells. For example, Ly49H recognizes the m157 glycoprotein encoded by mouse cytomegalovirus (MCMV).³.⁴ During NK cell development in the bone marrow, Ly49 receptors are acquired in a stochastic fashion just before cells undergo a major proliferative burst and are released into the periphery. Humans and mice with selective NK cell deficiencies are susceptible to severe recurrent infections, especially from herpesviruses like CMV.⁵.6

MicroRNAs (miRNAs) are ~22 nt noncoding RNAs generated from long RNA precursors by serial cleavage steps mediated by the Drosha-DGCR8 complex and Dicer. NK and T cells that lack miRNAs due to the targeted inactivation of *Dicer*, *Drosha*, or *DGCR8* show dramatic defects in proliferation, survival, and effector function. In addition, mutations in specific miRNAs such as miR-181, miR-150, and miR-155 can have dramatic effects on NK cell development, cytotoxicity and IFN- γ production. Individual miRNAs can modestly affect the stability and translation of hundreds of target mRNAs. Because multiple miRNAs may regulate the same

biological processes, post-transcriptional regulation of miRNAs as a class may profoundly alter gene expression programs.¹⁴

Eri1 is a 3'-to-5' exoribonuclease of the DEDDh family with a deeply conserved role in 5.8S rRNA 3' end processing. 15,16 It has also been repeatedly recruited into species-specific small RNA regulatory pathways over the course of evolution. *eri1* mutant *S. pombe* accumulate excess endogenous short interfering RNAs (endo-siRNAs) that promote heterochromatin formation. 17,18 In contrast, *C. elegans* ERI-1 forms a complex with Dicer that generates worm-specific classes of endo-siRNAs. 19,20 *eri-1* mutant worms lack these endo-siRNAs, but also display an enhanced RNAi (Eri) phenotype whereby exogenous siRNAs show more robust silencing of mRNA targets. 21 Eri1 overexpression suppresses RNAi in mouse and human cell lines, 22 but its role in mammalian endogenous small RNA pathways remains undefined. Here we report that Eri1 negatively regulates global miRNA abundance and is required to promote normal NK cell homeostasis and immune function.

METHODS

Mice and infections. C57BL/6 (JAX) (B6), CD45.1+ ($Ptprc^{a/a}$) B6 (NCI), ICR, and $Rag2^{-/-}ll2rg^{-/-}$ mice (Taconic) were purchased. $Eri1^{fl/fl}$; CD4-cre, $Eri1^{-/-}$, and Ly49H-deficient ($Klr8^{-/-}$) B6 mice were described previously. ^{15,23} ICR/B6 were generated by crossing ICR to $Eri1^{+/-}$ B6 mice and backcrossing F_1 mice to $Eri1^{+/-}$ B6. To create chimeras, embryonic day 14.5 fetal liver cells were harvested and injected i.v. into B6 mice lethally irradiated with a split dose of 1100 rad. For infections, mice were

injected i.p. with $5x10^4$ pfu MCMV (Smith Strain). All experiments were conducted in accordance with the University of California San Francisco Institutional Animal Care and Use Committee guidelines with approval from the university IACUC.

NK cytokine production and cytotoxicity. Splenic NK cells were stimulated with antibodies against NK1.1, NKp46, Ly49D, Ly49H, or rat IgG2a or were incubated with IL-12 (20 ng/ml) and IL-18 (10 ng/ml) (R&D Systems). For LAMP-1 analysis, stimulated NK were incubated with anti-CD107a antibody (1D4B eBioscience). Splenocytes were incubated on antibody-coated plates for 5 h in the presence of Brefeldin A (BFA) followed by intracellular cytokine staining for IFN- γ . For cytotoxicity assays wildtype (WT) and $Eri1^{-/-}$ NK1.1+ TCR β - NK cells were incubated for 6 h with Ba/F3 cells or Ba/F3 cells stably expressing m157.3 51Cr release was used as described to measure NK-mediated lysis.²⁴

Western blot. Splenic NK1.1+ TCR β - Ly49H+ cells from uninfected or MCMV-infected B6 mice were sorted using a FACSAria (BD). Western blots were performed using a monoclonal antibody against β -actin (AC-74, Sigma Aldrich) and an affinity purified polyclonal antibody against Eri1 (A28).¹⁵

Adoptive transfers. Congenically marked WT and $\it{Eri1-/-}$ B6 splenic Ly49H+ NK cells were mixed at a 1:1 ratio, labeled with 10 μ M CellTrace Violet as per manufacturer's instructions (Invitrogen), and 60,000 Ly49H+ NK equivalents were transferred i.v. into Ly49H-deficient recipients. Twenty-four h later, mice were

injected with MCMV. Alternatively, WT and $Eri1^{-/-}$ B6 splenic NK cells were mixed at a 1:1 ratio, and 0.5×10^6 NK equivalents were transferred i.v. into $Rag2^{-/-}ll2rg^{-/-}$ B6 mice.

MCMV titers. Unmixed chimeras were infected with MCMV and sacrificed 3.5 d later. Splenic and hepatic viral titers were determined as described previously.²⁴

T cell culture and stimulation. CD4+ T cells were purified from spleen and lymph nodes by magnetic bead selection (Dynal, Invitrogen) and activated with anti-CD3 and anti-CD28 antibodies. Cells were taken off stimulus on d 3 and expanded in IL-2-containing media for sorting and analysis on d 6. Splenic T cells from MCMV-infected mice (d 8 post-infection (p.i.)) were isolated and stimulated with MCMV peptides (Table S1) or 10 nM phorbol 12-myristate 13-acetate (PMA) and 1 μ M ionomycin as described previously.²⁵ Intracellular IFN- γ was analyzed as described above for NK cells.

MicroRNA microarrays. Purified CD4+ T cells from one *Eri1*-/- and two *Eri1*fl/fl; *CD4-cre* mice and WT littermate controls (*Eri1*+/+, *Eri1*fl/fl, and *Eri1*+/+; *CD4-cre*) were activated *in vitro* for 40 h under Th2 (1000 U/ml IL4 and, 5 μg/ml anti-IFN-γ) conditions. Total RNA was isolated (miRNeasy kit, Qiagen) and used for miRNA analysis using custom one-color Agilent microarrays (8X15K Agilent UCSF Custom miRNA V3.1) containing sequences from Sanger miRBase version 11.26 For each set of 5 replicated probes across arrays, log₂-scale average intensities were determined,

corrected for background and quantile-normalized. False discovery rate was calculated as described.²⁷

Deep sequencing. Small (18–30 bp) RNA libraries were constructed from activated ICR/B6 WT and $Eri1^{-/-}$ CD4+ T cells and sequenced as described.²⁸ Adaptor sequences were trimmed from reads as described,²⁹ and all reads 15–30 nt were mapped to the mouse genome (UCSC mm8 assembly). Only sequences mapping to the genome with up to 2 mismatches were analyzed. Mouse small noncoding RNA annotations were compiled as described.³⁰ For genome-wide analysis, sequences were grouped into independent genomic loci as described,²⁹ and relative reads from each library were compared at every locus. Using an empirical Bayes method³¹ we determined that loci with a posterior probability greater than 0.9 of \geq 5-fold change were determined to have significant differential expression.

Accession numbers: Deep sequencing (GSE31920) and microarray (GSE32126) data are available in the Gene Expression Omnibus (GEO) database.

RESULTS

Peripheral deficiency and impaired bone marrow expansion of Eri1-/- NK cells

Compared with other tissues, Eri1 is highly expressed in mouse spleen and thymus, suggesting a role in the immune system. To determine whether the absence of Eri1 alters mature immune cell homeostasis, we evaluated splenocyte

population frequencies in wildtype (WT) and Eri1-deficient ($Eri1^{-/-}$) animals. The frequency and number of NK cells in the spleens of $Eri1^{-/-}$ animals was reduced by 50% compared to their WT siblings (Fig. 1A-B). Other lymphocyte populations were present at normal numbers. NK cell frequency was also significantly reduced in the liver (P < 0.01) and bone marrow (BM; P < 0.05) (Fig. 1C). Similar results were obtained in hematopoietic chimeras reconstituted with WT or $Eri1^{-/-}$ E14.5 fetal liver cells (Fig. S1). Thus $Eri1^{-/-}$ NK cell reduction is intrinsic to the hematopoietic compartment.

We next considered the possibility that the decrease in *Eri1*-/- NK cells results from dysfunction in other hematopoietic cells. To test this hypothesis, we generated chimeras using a 1:1 mixture of *Eri1*+/+ (CD45.1+CD45.2+) and *Eri1*-/- (CD45.1-CD45.2+) E14.5 fetal liver cells. Mixed chimeras contained similar frequencies of BM *Eri1*+/+ and *Eri1*-/- Lin-Sca-1+c-Kit+ early hematopoietic precursors (Fig. 1D); yet, we observed a significant reduction in all splenic *Eri1*-/- lymphocyte lineages, including but not limited to NK cells (Figs. 1D-E). In contrast, *Eri1*+/+ and *Eri1*-/- splenic myeloid cell frequencies were similar. Since the presence of WT hematopoietic cells did not rescue the reduction in *Eri1*-/- NK cells, we conclude that Eri1 is required in a cell-intrinsic manner to maintain normal NK cell numbers. Furthermore, competitive reconstitution unmasked a general defect in *Eri1*-/- lymphocyte homeostasis that was not apparent in *Eri1*-/- mice (Fig. 1A-B). This may reflect defective peripheral turnover due to competition for limiting growth factors or reduced development from a common lymphocyte precursor.

Developing BM NK cells undergo ordered stages of maturation marked by the upregulation or downregulation of specific integrins and the acquisition of NK receptors.³² We examined five discrete populations of developing *Eri1*/** and *Eri1-/-* BM NK cells in mixed fetal liver chimeras (Figs. 1F and S2A). There were no differences in the relative frequencies of *Eri1*/** and *Eri1-/-* cells among early NK cell precursors (stages I-III). However, *Eri1-/-* NK cells were significantly reduced starting at stage IV, which corresponds with a major proliferative phase, and at stage V, which is equivalent to mature CD11b* NK cells. Though an underlying mechanism remains unclear, these data indicate that inefficient production of *Eri1-/-* NK cells in the BM contributes to their inability to populate peripheral compartments at normal frequencies.

Further analysis of developing WT BM NK populations revealed that stage III NK cells displayed high rates of cell death and apoptosis before they upregulated CD49b and underwent a major proliferative burst at stage IV (Fig. S2B-D). WT and $Eri1^{-1/-1}$ NK populations displayed similar frequencies of dead and apoptotic cells during all stages of BM development (Fig. S2B-C). Eri1 deficiency also did not affect the frequency of BrdU-labeled cells following a 3 or 16 hr pulse (Fig. S2D and data not shown). Rapid clearance of necrotic and apoptotic cells *in vivo* may preclude the detection of subtle differences in cell death, and differences in proliferation that occur outside the pulse window may not be detected by BrdU labeling. Nevertheless, we can exclude the possibility that major stage-specific differences in cell death and proliferation underlie the cell-intrinsic reduction of $Eri1^{-1/-1}$ BM NK cells.

Given the relatively large reduction in peripheral NK cell numbers compared with the BM, we tested whether $Eri1^{-/-}$ NK cells have a homeostatic defect that exists independently of developmental impairment. WT and $Eri1^{-/-}$ NK cells incorporated BrdU provided in drinking water at the same rate, indicating normal NK cell turnover at steady state $in\ vivo$ (Fig. S3A). $Eri1^{-/-}$ NK cells also expanded at the same rate as WT cells when transferred into lymphocyte-deficient $Rag2^{-/-}ll2rg^{-/-}$ mice (Fig. S3B). Constitutive signaling through the IL-15 receptor is essential for NK cell development and survival. WT and $Eri1^{-/-}$ NK cells cultured in IL-15 $ex\ vivo$ proliferated rapidly and underwent similar rates of cell death upon IL-15 withdrawal (Fig. S3C-D). Thus $Eri1^{-/-}$ NK cells are competent to signal through the IL-15 receptor and are not particularly sensitive to the pro-apoptotic effects of IL-15 withdrawal. Together these data suggest that $Eri1^{-/-}$ NK cells undergo impaired production in the BM in the setting of normal peripheral turnover and IL-15-dependent proliferation.

Impaired maturation and Ly49 receptor expression in Eri1-deficient NK cells

We examined the cell surface phenotype of *Eri1*-/- and WT NK cells in mixed chimeras to determine whether Eri1 deficiency affects NK cell maturation or activation status (Fig. 2A). *Eri1*-/- NK expressed normal levels of the activating receptors NK1.1 and NKp46, which are used to identify NK cells. They also expressed normal levels of NKG2D and CD69, which are upregulated acutely in activated cells, and KLRG1, which remains elevated on NK cells previously expanded by activation.³⁴ A significantly higher frequency of *Eri1*-/- NK cells expressed the

immature cell markers CD27 and NKG2A/C/E, and fewer *Eri1*-/- NK cells expressed CD49b and CD11b, two integrins upregulated in the final stages of NK cell maturation. Similar expression patterns were observed in *Eri1*-/- NK cells from unmixed chimeras (data not shown).

Eri1-deficient NK cells also displayed a skewed Ly49 receptor repertoire (Fig. 2B). Surprisingly, $Eri1^{-/-}$ NK cell populations displayed a specific reduction in the frequency of Ly49H and Ly49D-expressing cells. In contrast to these activating receptors, the inhibitory receptors Ly49C/I, Ly49G2, and Ly49A were expressed normally. Within each Ly49+ subset, WT and $Eri1^{-/-}$ NK cells displayed no difference in the intensity of Ly49 receptor staining. Since activating Ly49 receptors are more frequently expressed on mature than immature NK cells, we considered the possibility that reduced Ly49H expression frequency could simply reflect the altered maturation status of $Eri1^{-/-}$ NK cells. However, Ly49H expression was decreased among both mature CD11b+ and immature CD11b- $Eri1^{-/-}$ NK cells (Fig. 2C), indicating that this defect may occur independently of NK cell maturation.

During their development, NK cells acquire Ly49 receptors in response to signals from the BM stroma. To determine when in NK cell development $Eri1^{-/-}$ NK cells first show reduced Ly49H expression, we measured Ly49H+ NK cell frequencies among stage II-V cells in the BM of mixed chimeras. Immature CD49b- α_V + NK cells acquire Ly49 receptors as they upregulate c-Kit, which demarcates the transition from stage II to III cells (Fig. S2A). $Eri1^{-/-}$ NK cells showed a marked reduction in Ly49H+ NK frequency at each developmental stage (Fig. 2D).

decreased in stage III *Eri1*-/- NK cells, including inhibitory receptors (Table 1). The inhibitory Ly49 repertoire normalizes in peripheral *Eri1*-/- NK cells, perhaps reflecting a selective growth advantage for NK cells with specific Ly49 repertoires. Together these data indicate that peripheral *Eri1*-/- NK populations have an immature cell surface phenotype and a skewed Ly49 repertoire with fewer Ly49 activating receptors.

Eri1 is dispensable for Ly49H-dependent NK cell-mediated cytotoxicity

Activated NK cells degranulate and produce large amounts of IFN-y. We measured IFN-γ production and the degranulation marker LAMP-1 (CD107a) in freshly isolated splenocytes activated with inflammatory cytokines or plate-bound antibodies that ligate activating NK receptors. WT and *Eri1-/-* cells from mixed chimeras were stimulated together, negating indirect feedback mechanisms on NK cell activation. WT and Eri1-deficient NK cells showed similar LAMP-1 staining in all conditions tested except for ligation of Ly49H (Figs. 3A). In contrast, *Eri1-/-* NK cells displayed modestly reduced IFN-y expression upon crosslinking of all immunoreceptor tyrosine-based activation motif (ITAM)-associated receptors tested (Fig. 3B). More significant decreases were observed with Ly49H and Ly49D crosslinking (35% and 20%, respectively). These results likely reflect the reduced frequency of *Eri1-/-* NK cells expressing these receptors rather than specific effects on Ly49 signaling. Indeed, starting Ly49H+ NK cell frequency significantly correlated with both LAMP-1 and IFN-γ induction by Ly49H, but not NKp46 crosslinking (Figs. 3C-E). In addition, a consistent \sim 35% reduction in the frequency of IFN- γ -producing NK cells was observed when the Ly49H crosslinking antibody stimulus was titrated down over two orders of magnitude (data not shown).

To test whether *Eri1-/-* NK cells can efficiently kill target cells in a Ly49H-dependent manner, we incubated freshly isolated NK cells *ex vivo* with Ba/F3 cells stably transduced with the MCMV Ly49H ligand m157. WT and *Eri1-/-* NK cells lysed the parental Ba/F3 line at similar rates (Fig. 4A). Furthermore, WT and *Eri1-/-* Ly49H+ NK cells lysed Ba/F3-m157 targets at equal efficiency (Fig. 4B). Together these data indicate that *Eri1-/-* NK cells are competent to signal through NK cell receptors and mediate normal Ly49H-dependent and -independent cytotoxicity. However, the reduced frequency of Ly49H+ cells in *Eri1-/-* NK cell populations leads to proportional defects in Ly49H-dependent effector activities.

Eri1-/- NK cells expand less during MCMV infection and show poor control of viral load

Ly49H+ NK cells are critical for controlling MCMV infection in B6 mice.^{37,38}

Given the reduced Ly49H expression in *Eri1*-/- NK cell populations, we investigated the *in vivo* activation of *Eri1*-/- NK cells by MCMV. Early in MCMV infection all NK cells are activated nonspecifically by proinflammatory cytokines such as IL-12, IL-18, and type I interferons.^{39,40} Then, several days after infection, there is marked expansion of Ly49H+ NK cells driven directly by Ly49H ligation by the viral antigen m157.^{3,4} Eri1 is strongly upregulated in Ly49H+ NK cells over the course of MCMV infection (Fig. 5A), suggesting a potential role in NK cell activation. To study *Eri1*-/-NK cell activation in response to MCMV, we infected mixed chimeras, obviating

discrepant cytokine environments or antigenic loads that could complicate experiments in separate WT and $Eri1^{-/-}$ mice.

Early in MCMV infection, both WT and *Eri1*-/- NK cells responded with robust IFN-γ production (Fig. 5B) and upregulation of NKG2D and CD69 (Fig. 5C). These results are consistent with efficient IFN-γ production upon IL-12 and IL-18 stimulation *ex vivo* (Fig. 3B). Later in MCMV infection, WT Ly49H+ NK cells showed robust expansion, peaking at day 7 in both spleen and liver (Fig. 5D). In contrast, *Eri1*-/- Ly49H+ NK cells underwent inefficient expansion. As expected, Ly49H- NK cells showed little change in total cell number regardless of their genotype. To assess *Eri1*-/- NK cell expansion independent of the reduced initial Ly49H+ cell frequency, we adoptively transferred equal numbers of CellTrace Violet-labeled WT and *Eri1*-/- Ly49H+ NK cells into Ly49H-deficient hosts. Four days after infection with MCMV, WT Ly49H+ NK cells had diluted the cell proliferation dye more and undergone greater expansion than *Eri1*-/- cells (Fig. 5E-F). Thus, Eri1-deficient NK cells are activated normally in early MCMV infection yet undergo poor Ly49H-dependent proliferation as the infection progresses.

To determine if Eri1 is required to control viral load, we infected unmixed chimeras with MCMV. As observed in mixed chimeras, *Eri1*-/- NK cells showed robust expression of IFN-γ and upregulated the early activation markers CD69 and NKG2D yet displayed reduced expansion of Ly49H+ cells (data not shown). Like other mice with poor NK cell expansion,^{6,23} *Eri1*-/- chimeras exhibited decreased splenomegaly and increased viral titers (Fig. 5G-H). We conclude that Eri1 is required in a cell-intrinsic manner for the normal expansion of Ly49H+ NK cells and

control of MCMV infection.

Reduced virus-specific T cell responses in the absence of Eri1

Unlike NK cells, CD4 and CD8 lineage T cells were present at normal steady-state numbers and proportions in the thymus and peripheral lymphoid tissues of $Eri1^{-/-}$ fetal liver chimeras (data not shown and Fig. S1A). The proportions of naïve, memory and regulatory T cells were also normal, and similar results were obtained in $Eri1^{fi/fi}$; CD4-cre mice that lack Eri1 only in T cells (data not shown). However, given the more general defect in $Eri1^{-/-}$ lymphocyte development revealed in mixed fetal liver chimeras and the decreased expansion of antigen-specific $Eri1^{-/-}$ NK cells during MCMV infection, we examined MCMV-specific responses in $Eri1^{-/-}$ CD4+ and CD8+ T cells in mixed fetal liver chimeras.

At day 8 p.i., T cells were evaluated by flow cytometry and by restimulation *ex vivo* with immunodominant MCMV peptides.^{25,41} As expected, infection increased the overall frequency of CD8+ T cells (Fig. 6A) and the proportion of activated CD4+ and CD8+ T cells marked by high expression of CD44 and/or downregulation of CD62L (Fig. 6B). These changes occurred similarly in WT and *Eri1*-/- T cells (Fig. 6A-B). However, fewer *Eri1*-/- CD8+ cells were specific for the H2-Db-restricted M45₉₈₅-993 peptide epitope (Fig. 6C). Accordingly, M45 induced fewer IFN-γ-producing *Eri1*-/- CD8+ cells, despite their increased response to PMA and ionomycin (Figs. 6D-E). We also detected a reduced frequency of MCMV-specific IFN-γ-producing *Eri1*-/- CD4+ T cells despite robust IFN-γ production upon PMA and ionomycin restimulation (Figs. 6F-G). Together these data indicate that, like NK cells, *Eri1*-/- T

cells have diminished antigen-specific responses to MCMV infection. This defect is unlikely to contribute to poor MCMV control in *Eri1*-/- chimeras at d 3 p.i. (Fig. 5H), when T cells, as well as B and NKT cells, are dispensable for viral clearance.⁴² However, decreased anti-viral T cell responses in the absence of Eri1 may have important functional consequences for the control of latent infection and the establishment of MCMV-specific immunological memory.

Eri1 negatively regulates miRNA abundance in lymphocytes

We next sought to identify important RNA targets for Eri1 in mouse lymphocytes. Eri1 inhibits RNAi in worms and mammalian cell lines and degrades siRNA duplexes *in vitro*.^{21,22} Given structural similarities between miRNA and siRNA duplexes, we conjectured that Eri1 regulates miRNA abundance in lymphocytes. Indeed, quantitative real time PCR (qRT-PCR) revealed, on average, a 2-fold increase in miRNA expression in *Eri1*-/- NK cells compared to littermate controls (Fig. 7A). Highly expressed miRNAs (e.g. miR-150 and miR-21) and those expressed at one to two lower orders of magnitude (e.g. miR-106a and miR-181) were affected.⁴³ Other non-coding RNAs, including U6 snRNA, U7 snRNA, Arg-tRNA and Sno202 were unaffected (Fig. 7A and data not shown).

Eri1 also regulated miRNA abundance in CD4+ T cells. Northern blot analyses showed a modest, consistent increase in the expression of several miRNAs in Eri1-deficient T cells (Fig. 7B). Because we could transduce primary *Eri1-/-* T cells more easily than NK cells, we used these lymphocytes to rescue miRNA levels by ectopic expression of Eri1. Transducing Eri1-deficient T cells with a retrovirus encoding an

Eri1-ECFP fusion protein¹⁵ reduced miRNA expression to WT levels (Fig. 7C). Thus, altered miRNA abundance in Eri1-deficient lymphocytes was not the indirect result of impaired lymphocyte development.

To test whether Eri1 preferentially affects some miRNAs, we performed microarray analysis of three independent Eri1-deficient and matched WT control T cell samples (Fig. 7D). Despite a high degree of reproducibility between samples (Pearson correlation coefficient $r \ge 0.99$), this analysis revealed no differentially expressed miRNAs in Eri1-deficient cells when using a false discovery rate of 5%. Note that array data were quantile normalized to compare expression of each miRNA relative to all other miRNAs, so these experiments do not detect global changes in miRNA expression. The high degree of similarity in miRNA expression patterns between WT and Eri1-deficient T cells indicated that Eri1 globally regulates the homeostasis of all miRNAs without any discernible sequence specificity.

In *C. elegans*, Eri1 interacts with Dicer to form a complex that is required to generate some classes of endo-siRNAs.^{19,20} To determine if Eri1 is required for the biogenesis of any non-canonical classes of small RNAs in mouse lymphocytes, we used deep sequencing to broadly profile the small RNA transcriptome of WT and $Eri1^{-/-}$ T cells (Fig. 7E and Fig. S4). All sequences were mapped to the mouse genome and assigned to 390,000 empirically determined genomic loci as described previously.²⁹ This analysis revealed a high degree of similarity between WT and $Eri1^{-/-}$ small RNA libraries (r > 0.97) (Fig. 7E). Only two genomic loci had a greater than 90% probability of a 5-fold or greater expression difference between the two

libraries. A 5-fold cutoff for significance was established based on the observation that *C. elegans* deficient in components of the Eri1-Dicer complex show at least a 5-fold decrease in specific classes of endo-siRNAs.⁴⁴ Of the two loci differentially expressed in Eri1-deficient T cells, one (chromosome 13) could be accounted for by a SNP present in the *Eri1-/-* but not the WT sample. The other locus (chromosome 8) contained a 28 nt RNA that mapped to a non-conserved intronic region of *Ell*. Using qRT-PCR, we could not confirm that this RNA was differentially expressed in *Eri1-/-* T cells (data not shown). Together our small RNA profiling data show that Eri1 negatively regulates miRNA abundance in a sequence-independent manner and that Eri1 is not required for the biogenesis of any abundant classes of small RNAs in T cells.

DISCUSSION

Eri1 is a highly conserved exonuclease that has been recruited into small RNA regulatory pathways in evolutionarily diverse organisms. Our findings establish that mammalian Eri1 modulates global miRNA abundance, a novel regulatory activity that may be important for proper lymphocyte development and effector function. While $Eri1^{-/-}$ mice had normal numbers of B, T, and NKT cells, all $Eri1^{-/-}$ lymphocyte lineages were reduced in mixed fetal liver chimeras. Thus, in the absence of competition, the homeostatic control of peripheral B and T cell numbers in $Eri1^{-/-}$ mice likely masks a defect in their development. In contrast, steady-state NK cell populations were reduced to half their normal number. This observation may reflect differences in the regulation of NK cell versus B and T cell homeostasis,

or an NK cell-specific dependence on Eri1 activity. The remaining *Eri1-/-* NK cells exhibited an immature phenotype and skewed Ly49 repertoire marked by reduced Ly49H+ cells. Furthermore, these *Eri1-/-* Ly49H+ NK cells failed to expand efficiently during MCMV infection. *Eri1-/-* CD4+ and CD8+ T cells also displayed diminished antigen-specific MCMV responses, suggesting that Eri1 may generally enhance lymphocyte-mediated anti-viral immunity.

Immature BM CD49b⁻ α_{V} ⁺ NK cells acquire Ly49 receptors in a developmentally regulated fashion that correlates with c-Kit upregulation.³² Ly49 induction requires direct contact with the BM stroma and is altered in the setting of signaling pathway defects.^{35,36,45,46} Similar to NK cells deficient in PI3K subunits or phospholipase Cy2, $Eri1^{-/-}$ BM NK cells showed delayed acquisition of multiple Ly49 receptors. However, unlike these mutants, which show mirrored peripheral Ly49 reduction, $Eri1^{-/-}$ NK splenocytes have a normal Ly49 inhibitory repertoire and a selective reduction in Ly49D and Ly49H activating receptors. We hypothesize that the specific reduction in activating receptor repertoires results from delayed acquisition of all Ly49 receptors in the BM followed by the selective outgrowth of NK cells bearing specific inhibitory receptors.

Ly49A, Ly49C, Ly49I, Ly49G2, and Ly49D all recognize class I MHC, and MHC may in turn shape their expression on NK cells.⁴⁷ In contrast, the MCMV protein m157 is the only known ligand of Ly49H. The observed decrease in Ly49H and Ly49D-expressing *Eri1*-/- NK cells from mixed chimeras indicates that a cell-intrinsic mechanism underlies this defect rather than aberrant Ly49 ligand distribution. The adapter molecules DAP10 and DAP12 stabilize activating Ly49 receptors on the cell

surface, and loss of either of these proteins leads to reduced Ly49D and Ly49H expression.^{24,48} Yet receptor destabilization is an unlikely mechanism for Ly49 repertoire skewing on *Eri1*-/- NK cells, as they showed no change in receptor density at the cell surface. Another possibility is that Ly49 activating receptors are direct miRNA targets that become downregulated by miRNA derepression in *Eri1*-/- NK cells. This is also unlikely given that miRNA depletion from mature NK cells does not alter Ly49 expression.⁸ A more probable scenario is that Eri1 alters Ly49H and Ly49D acquisition indirectly through effects on Ly49 transcriptional regulators. Such a mechanism has been proposed for aberrant Ly49A acquisition observed in miR-150 mutant mice.⁹ Further study of *Eri1*-/- NK cells may provide new insight into the BM signals that drive Ly49 expression in developing NK cells.

The best predictor of effective antiviral immunity to MCMV in B6 mice is the expansion of pathogen-specific NK cells. 3,37,38,49 $Eri1^{-/-}$ NK cells displayed a reduced Ly49H+ repertoire and poor Ly49H-dependent expansion in response to viral infection, with a corresponding deficiency in viral clearance during the acute phase of infection. Though we observed a decreased frequency of MCMV-specific $Eri1^{-/-}$ T cells in mixed fetal liver chimeras, T, B, and NKT cells are dispensable for viral clearance during early acute infection. 42 Therefore, we speculate that NK cell dysfunction is the primary reason $Eri1^{-/-}$ chimeras poorly controlled MCMV viral load. However, we cannot rule out the possibility that other hematopoietic populations may contribute to diminished viral clearance. Further study is required to fully define the extent of Eri1 regulation of immune responses.

Reduced NK cell expansion was evident when equal numbers of WT and $Eri1^-$ /- Ly49H+ NK cells were transferred to Ly49H-deficient hosts, suggesting an NK cell-intrinsic defect. $Eri1^-$ /- NK cells also displayed a modest defect in IFN- γ production upon crosslinking of ITAM-associated receptors $in\ vitro$, suggesting a general defect in activating receptor signal transduction that may contribute to poor viral control. Yet on a per-cell basis, $Eri1^-$ /- and WT Ly49H+ NK cells surprisingly showed equal Ly49H-dependent degranulation and target cell killing. Thus, $Eri1^-$ /- NK cells are not generally hyporesponsive to Ly49H ligation or unable to mediate effector functions. Additionally, reduced NK cell expansion in MCMV infection does not reflect a general proliferation defect, as we observed normal IL-15-driven expansion $in\ vitro$ and $in\ vivo$. Further research is needed to identify the affected pathways that mediate poor expansion of $Eri1^-$ /- Ly49H+ NK cells during MCMV infection.

Though we do not yet understand how Eri1 modulates mature miRNA abundance, we speculate that it acts by direct enzymatic degradation of precursor or mature miRNAs, as is observed for the small RNA exonucleases SDN1 in *Arabidopsis* and XRN-2 in *C. elegans*. More generally, our data suggest that Eri1-dependent regulation of endogenous small RNAs in mammalian somatic cells is distinctly different from that observed in *S. pombe* or *C. elegans*, where Eri1 regulates endo-siRNA abundance. Deep sequencing analysis of small RNAs in WT and Eri1-deficient T cells revealed no small RNA species that were as dependent on Eri1 as some classes of endo-siRNAs are in *C. elegans*. Thus, miRNAs are likely the major small RNA target for Eri1 in somatic mammalian cells. This activity may not

be restricted to mammals, as one previous report found that *eri-1* mutant *C. elegans* expressed increased levels of mature miR-238.²⁰

We cannot exclude the possibility that other Eri1 substrates, such as ribosomal RNA, may mediate some of the phenotypes observed in *Eri1-/-* lymphocytes. Interestingly, *Eri1-/-* mice share some phenotypic similarities with humans who have Diamond-Blackfan anemia (DBA),¹⁵ a heterogeneous disease most commonly attributed to *RPS19* mutations.⁵² Lymphocyte deficiency is a common feature of many ribosomopathies including DBA, Shwachman-Diamond syndrome, and dyskeratosis congenita.⁵³ Of note, we were unable to detect NK cell homeostasis defects in *RPS19* mutant mice (*Dsk3*) or *RPS20* mutants (*Dsk4*).⁵⁴ Studies are currently underway to determine if NK cell deficiency occurs in other mouse strains with mutations in ribosome-associated proteins.

These results imply that miRNAs as a class are negatively regulated in lymphocytes and, by extension, so is miRNA-mediated gene silencing. Though Eri1 is broadly expressed due to its constitutive role in 5.8S rRNA maturation, it is enriched in lymphoid organs and is strongly upregulated in activated lymphocytes. Thus, Eri1-mediated repression of miRNAs may lead to cell-type specific defects. In this capacity, Eri1 comprises a growing class of factors that modulate miRNA expression at a global level. Many of these factors, including Eri1, are attractive therapeutic targets whose inhibition could enhance miRNA or siRNA-mediated gene repression.

Acknowledgements

The authors thank Ariya Lapan, Laura Smith, and Eric Yanni for technical assistance;

Chris Eisley, Rebecca Barbeau, Andrea Barczak, and David Erle (SABRE Functional

Genomics Core) for expert assistance with microarray experiments; Jon Woo (UCSF

Genomics Core Facility) for assistance with small RNA sequencing; Natalie Bezman

for critical comments on the manuscript; Joseph Sun, Sandra Lopez-Verges, Maelig

Morvan, and Yosuke Kamimura for helpful discussions. This work was supported by

the Burroughs Wellcome Fund (CABS 1006173), the NIH (HL109102 to K.M.A. and

AI089828, AI70788 and AI068129 to L.L.L.), the German Research Foundation (DFG

HE 3359/3-1) and the UCSF/NIH Medical Scientist Training Program (M.F.T.). L.L.L.

is an American Cancer Society Professor.

Authorship Contributions: M.F.T. and K.M.A. performed research, analyzed data

and wrote the paper. S.A.W. and M.P. performed some of the T cell experiments,

including miRNA qPCR for transduced T cells (S.A.W.), J.E.B., M.R. and P.W. assisted

with small RNA deep sequencing analysis and statistics. K.M.A. and M.F.T. designed

23

research with critical input from L.L.L. and V.H.

Conflict-of-interest disclosure: The authors have no financial conflict of interest.

REFERENCES

- 1. Vivier E, Tomasello E, Baratin M, Walzer T, Ugolini S. Functions of natural killer cells. *Nat Immunol.* 2008;9(5):503-510.
- 2. Lanier LL. Up on the tightrope: natural killer cell activation and inhibition. *Nat Immunol.* 2008;9(5):495-502.
- 3. Arase H, Mocarski ES, Campbell AE, Hill AB, Lanier LL. Direct recognition of cytomegalovirus by activating and inhibitory NK cell receptors. *Science*. 2002;296(5571):1323-1326.
- 4. Smith HR, Heusel JW, Mehta IK, et al. Recognition of a virus-encoded ligand by a natural killer cell activation receptor. *Proc Natl Acad Sci U S A*. 2002;99(13):8826-8831.
- 5. Biron CA, Byron KS, Sullivan JL. Severe herpesvirus infections in an adolescent without natural killer cells. *N Engl J Med*. 1989;320(26):1731-1735.
- 6. Bukowski JF, Woda BA, Welsh RM. Pathogenesis of murine cytomegalovirus infection in natural killer cell-depleted mice. *J Virol*. 1984;52(1):119-128.
- 7. O'Connell RM, Rao DS, Chaudhuri AA, Baltimore D. Physiological and pathological roles for microRNAs in the immune system. *Nat Rev Immunol*. 2010;10(2):111-122.
- 8. Bezman NA, Cedars E, Steiner DF, Blelloch R, Hesslein DG, Lanier LL. Distinct requirements of microRNAs in NK cell activation, survival, and function. *J Immunol*. 2010;185(7):3835-3846.
- 9. Bezman NA, Chakraborty T, Bender T, Lanier LL. miR-150 regulates the development of NK and iNKT cells. *J Exp Med*. 2011;208(13):2717-2731.
- 10. Cichocki F, Felices M, McCullar V, et al. Cutting edge: micro RNA-181 promotes human NK cell development by regulating Notch signaling. *J Immunol*. 2011;187(12):6171-6175.
- 11. Trotta R, Chen L, Ciarlariello D, et al. MiR-155 regulates IFN-gamma production in natural killer cells. *Blood*. 2012.
- 12. Baek D, Villen J, Shin C, Camargo FD, Gygi SP, Bartel DP. The impact of microRNAs on protein output. *Nature*. 2008;455(7209):64-71.
- 13. Selbach M, Schwanhausser B, Thierfelder N, Fang Z, Khanin R, Rajewsky N. Widespread changes in protein synthesis induced by microRNAs. *Nature*. 2008;455(7209):58-63.
- 14. Siomi H, Siomi MC. Posttranscriptional regulation of microRNA biogenesis in animals. *Mol Cell*. 2010;38(3):323-332.
- 15. Ansel KM, Pastor WA, Rath N, et al. Mouse Eri1 interacts with the ribosome and catalyzes 5.8S rRNA processing. *Nat Struct Mol Biol*. 2008;15(5):523-530.
- 16. Gabel HW, Ruvkun G. The exonuclease ERI-1 has a conserved dual role in 5.8S rRNA processing and RNAi. *Nat Struct Mol Biol*. 2008;15(5):531-533.
- 17. Bühler M, Verdel A, Moazed D. Tethering RITS to a nascent transcript initiates RNAi- and heterochromatin-dependent gene silencing. *Cell*. 2006;125(5):873-886.
- 18. Iida T, Kawaguchi R, Nakayama J. Conserved ribonuclease, Eri1, negatively regulates heterochromatin assembly in fission yeast. *Curr Biol.* 2006;16(14):1459-1464.

- 19. Duchaine TF, Wohlschlegel JA, Kennedy S, et al. Functional proteomics reveals the biochemical niche of C. elegans DCR-1 in multiple small-RNA-mediated pathways. *Cell*. 2006;124(2):343-354.
- 20. Lee RC, Hammell CM, Ambros V. Interacting endogenous and exogenous RNAi pathways in Caenorhabditis elegans. RNA. Vol. 12; 2006:589-597.
- 21. Kennedy S, Wang D, Ruvkun G. A conserved siRNA-degrading RNase negatively regulates RNA interference in C. elegans. *Nature*. 2004;427(6975):645-649.
- 22. Bühler M, Mohn F, Stalder L, Mühlemann O. Transcriptional silencing of nonsense codon-containing immunoglobulin minigenes. *Molecular Cell*. 2005;18(3):307-317.
- 23. Fodil-Cornu N, Lee SH, Belanger S, et al. Ly49h-deficient C57BL/6 mice: a new mouse cytomegalovirus-susceptible model remains resistant to unrelated pathogens controlled by the NK gene complex. *J Immunol*. 2008;181(9):6394-6405.
- 24. Orr MT, Sun JC, Hesslein DG, et al. Ly49H signaling through DAP10 is essential for optimal natural killer cell responses to mouse cytomegalovirus infection. *J Exp Med*. 2009;206(4):807-817.
- 25. Arens R, Wang P, Sidney J, et al. Cutting edge: murine cytomegalovirus induces a polyfunctional CD4 T cell response. *J Immunol*. 2008;180(10):6472-6476.
- 26. Griffiths-Jones S, Saini HK, van Dongen S, Enright AJ. miRBase: tools for microRNA genomics. *Nucleic Acids Res.* 2008;36(Database issue):D154-158.
- 27. Benjamini Y, Hochberg Y. Controlling the false discovery rate: A practical and powerful approach to multiple testing. *J Royal Stat Soc* 1995;57289-300.
- 28. Thomas MF, Ansel KM. Construction of small RNA cDNA libraries for deep sequencing. *Methods Mol Biol*. 2010;66793-111.
- 29. Babiarz JE, Ruby JG, Wang Y, Bartel DP, Blelloch R. Mouse ES cells express endogenous shRNAs, siRNAs, and other Microprocessor-independent, Dicerdependent small RNAs. *Genes Dev.* 2008;22(20):2773-2785.
- 30. Steiner DF, Thomas MF, Hu JK, et al. MicroRNA-29 Regulates T-Box Transcription Factors and Interferon-gamma Production in Helper T Cells. *Immunity*. 2011:35(2):169-181.
- 31. Wu Z, Jenkins BD, Rynearson TA, et al. Empirical bayes analysis of sequencing-based transcriptional profiling without replicates. *BMC Bioinformatics*. 2010;11564.
- 32. Kim S, lizuka K, Kang HS, et al. In vivo developmental stages in murine natural killer cell maturation. *Nat Immunol.* 2002;3(6):523-528.
- 33. Ma A, Koka R, Burkett P. Diverse functions of IL-2, IL-15, and IL-7 in lymphoid homeostasis. *Annu Rev Immunol*. 2006;24657-679.
- 34. Sun JC, Beilke JN, Lanier LL. Adaptive immune features of natural killer cells. *Nature*. 2009;457(7229):557-561.
- 35. Williams NS, Moore TA, Schatzle JD, et al. Generation of lytic natural killer 1.1+, Ly-49- cells from multipotential murine bone marrow progenitors in a stromafree culture: definition of cytokine requirements and developmental intermediates. *J Exp Med.* 1997;186(9):1609-1614.

- 36. Williams NS, Klem J, Puzanov IJ, Sivakumar PV, Bennett M, Kumar V. Differentiation of NK1.1+, Ly49+ NK cells from flt3+ multipotent marrow progenitor cells. *J Immunol*. 1999;163(5):2648-2656.
- 37. Lee SH, Girard S, Macina D, et al. Susceptibility to mouse cytomegalovirus is associated with deletion of an activating natural killer cell receptor of the C-type lectin superfamily. *Nat Genet*. 2001;28(1):42-45.
- 38. Brown MG, Dokun AO, Heusel JW, et al. Vital involvement of a natural killer cell activation receptor in resistance to viral infection. *Science*. 2001;292(5518):934-937.
- 39. Orange JS, Biron CA. Characterization of early IL-12, IFN-alphabeta, and TNF effects on antiviral state and NK cell responses during murine cytomegalovirus infection. *J Immunol*. 1996;156(12):4746-4756.
- 40. Pien GC, Satoskar AR, Takeda K, Akira S, Biron CA. Cutting edge: selective IL-18 requirements for induction of compartmental IFN-gamma responses during viral infection. *J Immunol*. 2000;165(9):4787-4791.
- 41. Munks MW, Gold MC, Zajac AL, et al. Genome-wide analysis reveals a highly diverse CD8 T cell response to murine cytomegalovirus. *J Immunol*. 2006;176(6):3760-3766.
- 42. Loh J, Chu DT, O'Guin AK, Yokoyama WM, Virgin HW. Natural killer cells utilize both perforin and gamma interferon to regulate murine cytomegalovirus infection in the spleen and liver. *J Virol*. 2005;79(1):661-667.
- 43. Fehniger TA, Wylie T, Germino E, et al. Next-generation sequencing identifies the natural killer cell microRNA transcriptome. *Genome Res.* 2010;20(11):1590-1604.
- 44. Gent JI, Lamm AT, Pavelec DM, et al. Distinct phases of siRNA synthesis in an endogenous RNAi pathway in C. elegans soma. *Mol Cell*. 2010;37(5):679-689.
- 45. Guo H, Samarakoon A, Vanhaesebroeck B, Malarkannan S. The p110 delta of PI3K plays a critical role in NK cell terminal maturation and cytokine/chemokine generation. *I Exp Med*. 2008;205(10):2419-2435.
- 46. Tassi I, Presti R, Kim S, Yokoyama WM, Gilfillan S, Colonna M. Phospholipase C-gamma 2 is a critical signaling mediator for murine NK cell activating receptors. *J Immunol*. 2005;175(2):749-754.
- 47. Salcedo M, Diehl AD, Olsson-Alheim MY, et al. Altered expression of Ly49 inhibitory receptors on natural killer cells from MHC class I-deficient mice. *J Immunol*. 1997;158(7):3174-3180.
- 48. Bakker AB, Hoek RM, Cerwenka A, et al. DAP12-deficient mice fail to develop autoimmunity due to impaired antigen priming. *Immunity*. 2000;13(3):345-353.
- 49. Daniels KA, Devora G, Lai WC, O'Donnell CL, Bennett M, Welsh RM. Murine cytomegalovirus is regulated by a discrete subset of natural killer cells reactive with monoclonal antibody to Ly49H. *J Exp Med*. 2001;194(1):29-44.
- 50. Ramachandran V, Chen X. Degradation of microRNAs by a family of exoribonucleases in Arabidopsis. *Science*. 2008;321(5895):1490-1492.
- 51. Chatterjee S, Grosshans H. Active turnover modulates mature microRNA activity in Caenorhabditis elegans. *Nature*. 2009;461(7263):546-549.

- 52. Willig TN, Draptchinskaia N, Dianzani I, et al. Mutations in ribosomal protein S19 gene and diamond blackfan anemia: wide variations in phenotypic expression. *Blood.* 1999;94(12):4294-4306.
- 53. Khan S, Pereira J, Darbyshire PJ, et al. Do ribosomopathies explain some cases of common variable immunodeficiency? *Clin Exp Immunol*. 2010;163(1):96-103.
- 54. McGowan KA, Li JZ, Park CY, et al. Ribosomal mutations cause p53-mediated dark skin and pleiotropic effects. *Nat Genet*. 2008;40(8):963-970.

Table 1. Activating and inhibitory receptor repertoire on splenic and developing bone marrow NK cells.

_	Eri1	II	III	IV	V	Spleen
Ly49H	+/+	1.3 (0.1) 0.5 (0.3)	11.0 (2.5) 4.6 (2.0)	59.6 (3.4) 40.8 (0.6)	76.7 (3.8) 61.4 (1.7)	71.0 (3.5) 50.1 (3.5)
Ly49D	+/+	2.8 (0.5)	13.6 (2.0)	54.6 (2.9)	55.4 (1.5)	59.2 (1.0)
	-/-	2.3 (0.7)	6.9 (1.8)	47.7 (1.8)	53.1 (1.6)	48.4 (1.4)
Ly49G2	+/+	4.2 (1.6)	15.9 (3.1)	50.4 (5.6)	49.2 (4.9)	37.3 (2.7)
	-/-	4.2 (1.6)	10.2 (2.4)	56.6 (2.3)	56.0 (5.2)	38.1 (6.0)
Ly49C/I	+/+	5.5 (0.7)	19.0 (4.9)	30.9 (1.2)	34.6 (1.1)	28.9 (3.5)
	-/-	3.5 (1.2)	7.4 (1.2)	26.0 (1.7)	30.9 (1.9)	24.4 (4.0)
NKG2A/C/E	+/+	59.8 (0.7) 60.7 (3.2)	60.1 (2.0) 60.0 (1.8)	44.9 (0.7) 55.9 (4.2)	45.5 (1.1) 51.8 (2.8)	44.0 (1.3) 52.2 (0.9)

WT CD45.1+ lethally irradiated hosts were reconstituted with a 1:1 mixture of fetal liver cells from congenic WT (CD45.1+ CD45.2+) and $Eri1^{-/-}$ (CD45.2+) mice and analyzed 12 weeks later. Table shows frequencies of NK cell receptor expression on freshly isolated WT and $Eri1^{-/-}$ splenic NK cells (NK1.1+ CD3 ϵ -) and stage II – V developing BM NK cells (gating strategy shown in Fig. S2A). Table lists mean (SD) for 3 mice.

FIGURE LEGENDS

Figure 1. NK cell deficiency in *Eri1-/-* **mice.** Frequency **(A)** and absolute number **(B)** of spleen T (CD3 ϵ + NK1.1-), B (CD19+), NKT (NK1.1+ CD3 ϵ +), NK (NK1.1+ CD3 ϵ -), and Mac1+ (CD11b+ NK1.1-) cells enumerated by flow cytometry (N=5 ICR/B6 mice). (C) NK1.1+ CD3e-NK cells in the indicated tissues. Numbers are NK cell frequency ± SD among total lymphocytes (N=5 ICR/B6 mice). (D - F) CD45.1+ lethally irradiated hosts were reconstituted with a 1:1 mixture of fetal liver cells from WT (CD45.1+ CD45.2+) and $Eri1^{-/-}$ (CD45.2+) donors and analyzed 8 – 15 weeks later (N=3). (D) Frequency of donor- and host-derived cells among BM LSK (Lineage-c-Kit+Sca-1+) cells and spleen CD45+, B, CD4+ and CD8+ T, NKT, NK, macrophage (CD11b+ NK1.1- Gr1-) and granulocyte (CD11b+ Gr1+) cells. (E) Frequency of donor- and host-derived cells among NK cells in the indicated tissues. **(F)** Frequency of developing NK cell subsets (see Fig. S2A for gating strategy) among BM WT (CD45.1+CD45.2+) and $Eri1^{-/-}$ (CD45.1-CD45.2+) cells. Bar graphs show mean \pm SD. *P \leq 0.05, unpaired (A-B) or paired (D-F) Student's T-test. All data are representative of at least two independent experiments.

Figure 2. Impaired maturation and Ly49 receptor expression in *Eri1*-/- NK. B6 WT CD45.1+ lethally irradiated hosts were reconstituted with a 1:1 mixture of congenic WT (CD45.1+ CD45.2+) and *Eri1*-/- (CD45.2+) fetal liver cells. Splenic (A-C) and BM (D) NK cells were analyzed by flow cytometry at 8-15 weeks. **(A)** Cell surface expression of activating receptors (NKp46 and NK1.1), activation markers (NKG2D and CD69) and maturation markers (CD27, NKG2A/C/E, KLRG1, CD11b

and CD49b) on WT (CD45.1+CD45.2+) and $Eri1^{-/-}$ (CD45.1-CD45.2+) cells (left). Gated NK1.1+ CD3 ϵ - cells are shown for all stains, except for NK1.1, which shows gating on NKp46+ TCR β -cells. Summary of markers with significantly different expression on WT and $Eri1^{-/-}$ NK cells (right). **(B)** Splenic NK cell activating and inhibitory Ly49 receptors. **(C)** Percentage of Ly49H+ cells among CD11b+ and CD11b- NK cells. **(D)** Percentage of Ly49H+ WT and $Eri1^{-/-}$ NK cells at various stages of NK cell maturation in the BM (gating shown in Fig. S2A). Bar graphs and flow cytometry plots show mean \pm SD (N=3 mice). *P \leq 0.05, paired Student's T-test.

Figure 3. Normal Ly49H-dependent NK cytotoxicity in the absence of Eri1. B6 WT CD45.1+ lethally irradiated hosts were reconstituted with a 1:1 mixture of congenic WT (CD45.1+ CD45.2+) and Eri1-/- (CD45.2+) fetal liver cells. (A) At 12 weeks, splenocytes were isolated and incubated in wells coated with IgG or mAbs against NK1.1, NKp46, Ly49D or Ly49H in the presence of anti-CD107a mAb. Alternatively, NK cells were stimulated with IL-12 and IL-18. Frequency of degranulated WT (CD45.1+CD45.2+) and Eri1-/- (CD45.1-CD45.2+) CD107a+ NK cells (CD49b+TCRβ-) is shown. (B) Splenic NK cells stimulated as in (A) in the presence of brefeldin A and stained for intracellular IFN-γ. Flow cytometry plots show mean values for 10 mice. Summary graphs for Eri1-/- NK (right) show mean relative to wildtype ± SD (paired Student's T-Test). (C-E) Regression of CD107a (C) or IFN-γ (D-E) expression on percentage of Ly49H+ NK cells following stimulation with indicated mAbs. The Pearson correlation coefficient (r) and significance test for non-

zero correlation (P) are shown for each plot (N=10 mice from three independent experiments).

Figure 4. Normal NK-mediated killing in the absence of Eri1. Lethally irradiated CD45.1+ mice were reconstituted with CD45.2+ B6 WT or *Eri1-/-* fetal liver cells. Ten weeks later, splenic NK cells pooled from 3-4 mice were incubated with ⁵¹Cr-labeled target Ba/F3 cells (A) or Ba/F3 cells stably expressing MCMV m157 (B). Error bars indicate SD for triplicate measurements. Data are representative of two independent experiments.

Figure 5. Eri1 is required for Ly49H+ NK cell expansion and control of viral titers in MCMV infection. (A) Anti-Eri1 mAb immunoblot of Ly49H+ NK cells
pooled from 3-4 mice and sorted at various time points after MCMV infection. Data
are representative of two independent experiments. **(B - D)** B6 WT CD45.1+ lethally
irradiated hosts were reconstituted with a 1:1 mixture of congenic WT (CD45.1+
CD45.2+) and *Eri1-/-* (CD45.2+) fetal liver cells. At 8 – 15 weeks, chimeras were
infected with MCMV. WT (CD45.1+CD45.2+) and *Eri1-/-* (CD45.1-CD45.2+) NK cells
(NK1.1+ CD3ε-) were analyzed for (B) intracellular IFN-γ and (C) cell surface CD69
and NKG2D expression. (D) Absolute numbers of WT and *Eri1-/-* Ly49H+ and Ly49HNK cells in the spleen and liver at various time points after infection. Error in (B)
and (D) indicate SD (N=3 mice). **(E - F)** CD45.2+ *Eri1-/-* splenic Ly49H+ NK cells from
reconstituted fetal liver chimeras or B6 mice were mixed 1:1 with splenic Ly49H+
NK cells from CD45.1+CD45.2+ or CD45.1+WT B6 mice. Mixed splenocytes were

labeled with CellTrace Violet and transferred into B6 CD45.1+ $Ly49H^{-/-}$ hosts. (E) CellTrace Violet dilution before and after MCMV infection. (F) Percentage of Ly49H+ NK cells transferred at day 0 (mean \pm SEM, N=13 infected and four uninfected mice from four independent experiments). **P \leq 0.001, paired Student's T-Test. (G-H) B6 WT CD45.1+ lethally irradiated hosts were reconstituted with CD45.2+ WT or $Eri1^{-/-}$ fetal liver cells and infected with MCMV at 12 weeks. (G) Absolute numbers of WT and $Eri1^{-/-}$ CD45.2+ splenocytes over the course of infection (mean \pm SD, N=3 mice). (H) Viral titers in the spleen and liver were determined at d 3.5 p.i. by plaque assays. Horizontal line indicates the mean of each group (N=3 mice). *P \leq 0.05, two-tailed Mann-Whitney U test.

Figure 6. Reduced MCMV-specific CD4+ and CD8+ T cell frequency in the absence of Eri1. B6 WT CD45.1+ lethally irradiated hosts were reconstituted with a 1:1 mixture of congenic WT (CD45.1+ CD45.2+) and Eri1-/- (CD45.2+) fetal liver cells. At 8 – 15 weeks, chimeras were infected with MCMV and splenocytes were analyzed by flow cytometry at day 8 p.i. (A) Frequency of CD4+ and CD8+ cells among WT (CD45.1+ CD45.2+) or Eri1-/- (CD45.1- CD45.2+) splenocytes. (B) CD44 and CD62L expression on WT and Eri1-/- CD4+ and CD8+ cells. (C) Frequency of WT and Eri1-/- (day 8 p.i.) or WT control (uninfected) CD8+ cells labeled with M45-loaded H2-Db:Ig dimer. (D-G) Splenocytes from infected mice were restimulated with indicated peptides or PMA and ionomycin. Flow cytometric plots show the average percentage of gated CD8+ (D) or CD4+ (F) cells producing intracellular IFN-γ. Summary graphs for Eri1-/- splenic CD8+ (E) and CD4+ (G) T cells show mean IFN-γ

expression relative to WT. Numbers indicate average values \pm SD (A-C) or SEM (E and G) for 6 mice from two independent experiments. *P \leq 0.05 **P \leq 0.001, unpaired Student's T-Test.

Figure 7. Eri1 negatively regulates miRNAs in lymphocytes. (A) qRT-PCR analysis of miRNA expression in ICR/B6 $Eri1^{-/-}$ NK (NK1.1+ CD3 ϵ^-) cells purified by flow cytometry. Left, miRNA levels in *Eri1*-/- NK cells shown relative to WT (light gray bars). Right, sum of measurements from ten miRNAs (dark gray bar) and Sno 202 (white bar). Data were normalized to U6 snRNA. Graphs indicate mean ± SEM (N=6 ICR/B6 littermates). (B) Northern blot analysis of miRNAs from Eri1 wildtype (WT, *Eri1*+/+;*CD4*-*cre*), heterozygous (Het, *Eri1*fl/+;*CD4*-*cre*), and knockout (KO, Eri1f^{1/fl};CD4-cre) CD4+ T cells. Values indicate miRNA-specific signals quantified by phosphorimager, normalized to Arg-tRNA, and expressed relative to WT T cells. (C) Left, qRT-PCR analysis of miRNA expression in Eri1-deficient (Eri1^{f1/fl};CD4-cre) T cells transduced with retroviruses encoding Thy 1.1 and ECFP (light gray bars) or Thy 1.1 and Eri 1-ECFP (dark gray bars). Total RNA was prepared from transduced Thy 1.1+ T cells purified by FACS. Data were normalized to U6 snRNA and expressed relative to miRNA measured in WT ($Eri1^{+/+}$;CD4-cre) T cells transduced with ECFP retrovirus. Right, average of all miRNAs measured and Sno202 control. Columns show mean ± SEM (four independent experiments). (D) Microarray comparison of miRNA expression patterns in WT and Eri1-deficient CD4+T cells. Circles show average log₂ hybridization fluorescence intensity values for quantile-normalized data from three independent T cell samples. Black diagonal lines show 2-fold

intensity differences. **(E)** Small RNA read counts from WT and *Eri1-/-* T cell sequencing libraries. Dots show read counts at independent genomic loci with reads normalized to total genomic sequences in each library. Black lines indicate 5-fold expression differences. Circled dots show loci with > 90% posterior probability of a 5-fold expression difference between libraries. The location of these loci and gene origin of the most frequently cloned RNA from that locus are Chr13:98860450–98860650, *RPS18* pseudogene (left) and Chr8:73490090–73490290, *Ell* (right).



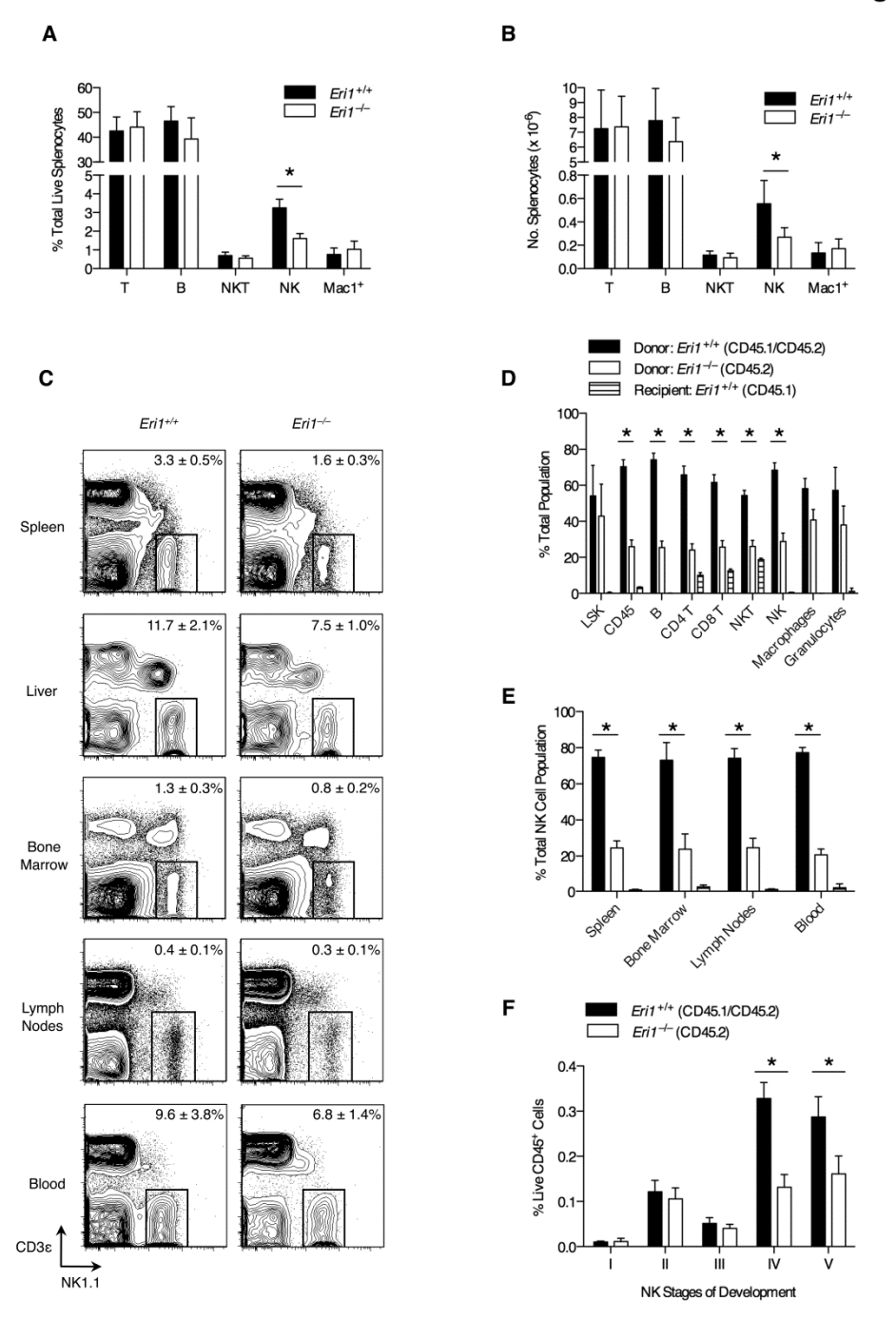


Figure 2

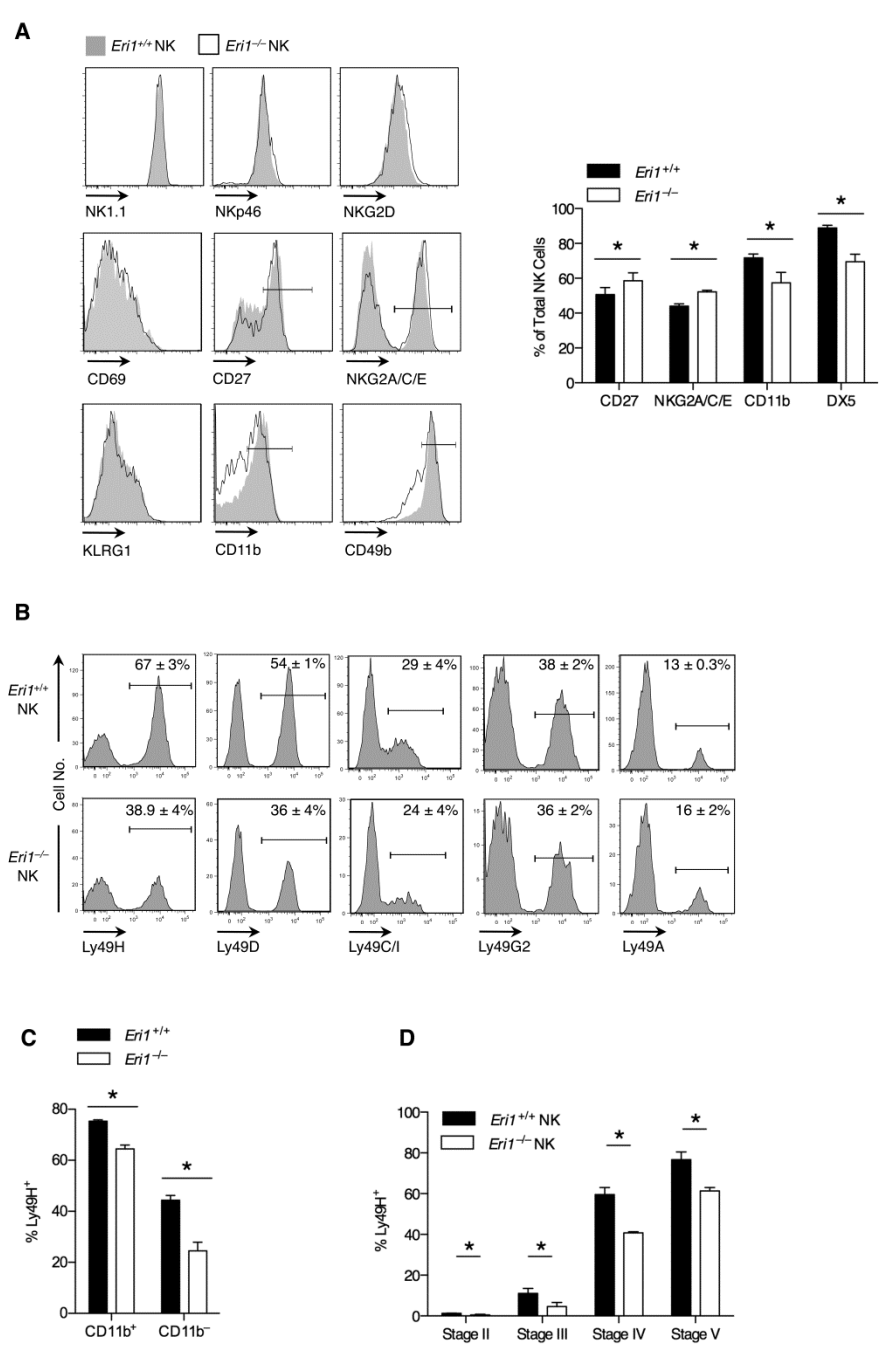


Figure 3

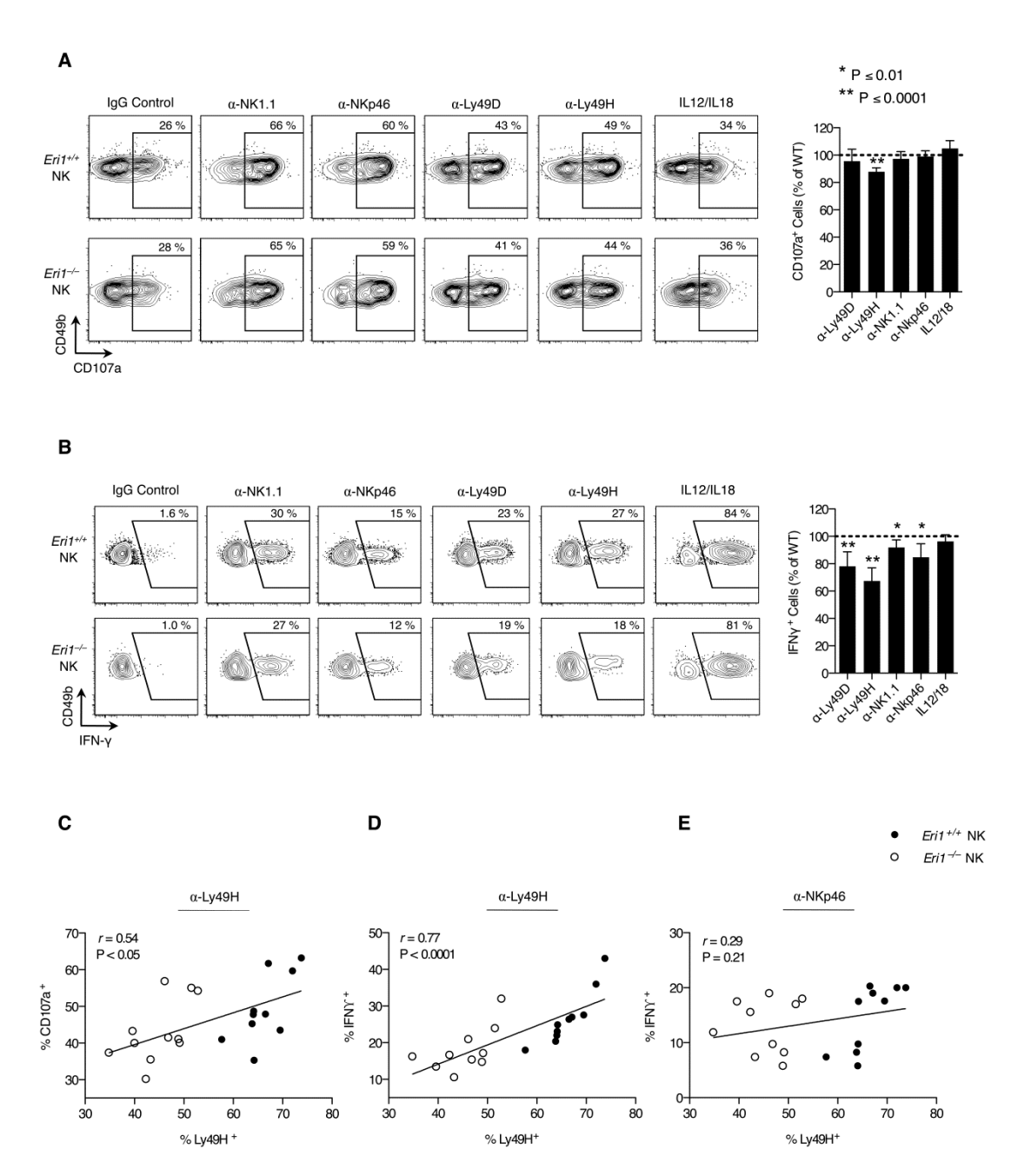
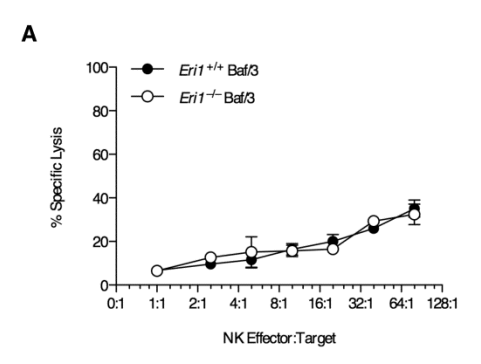


Figure 4



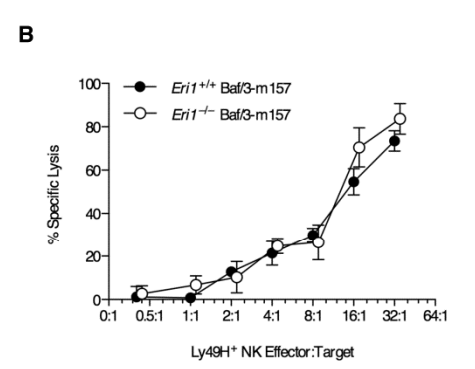


Figure 5

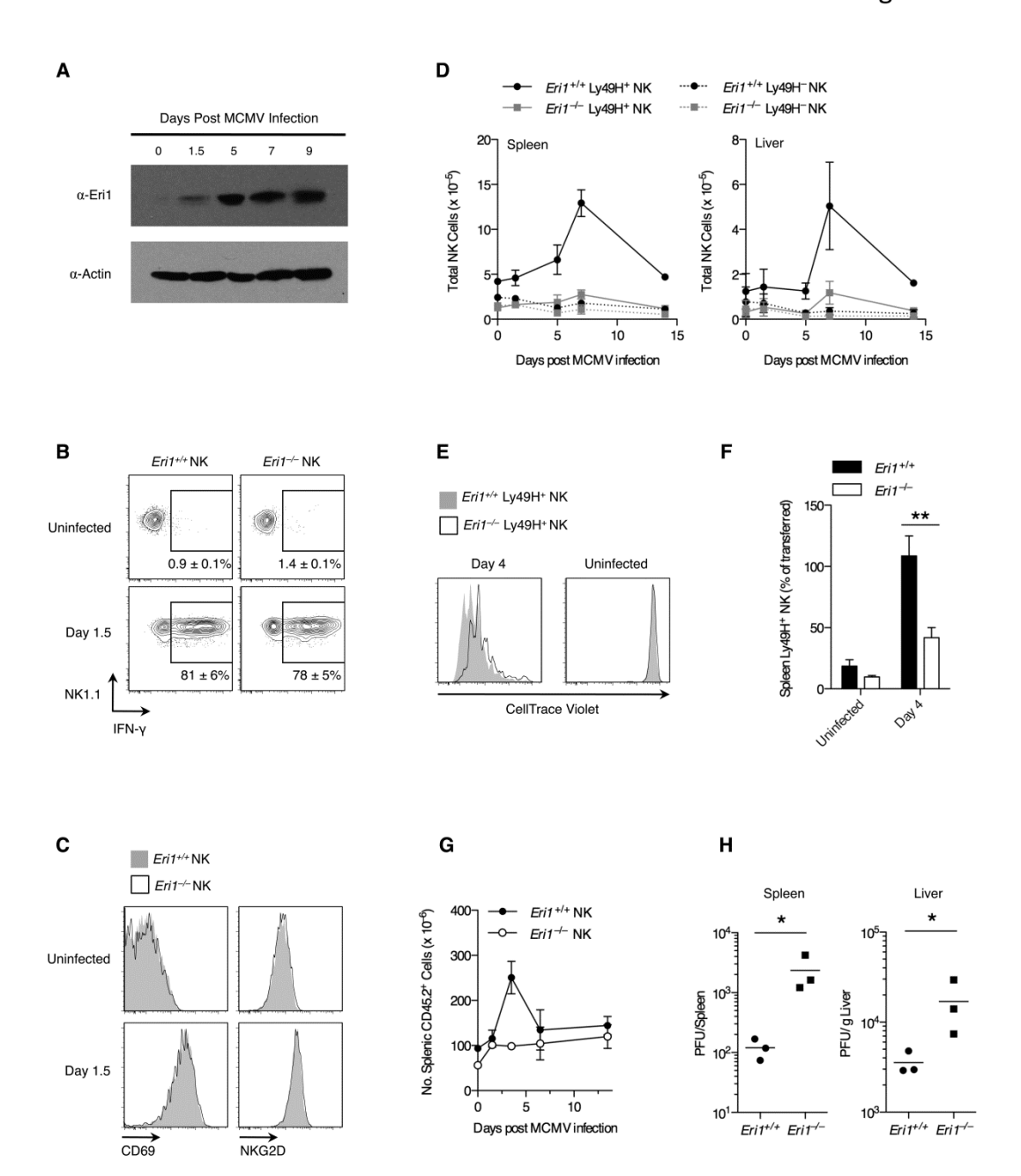


Figure 6

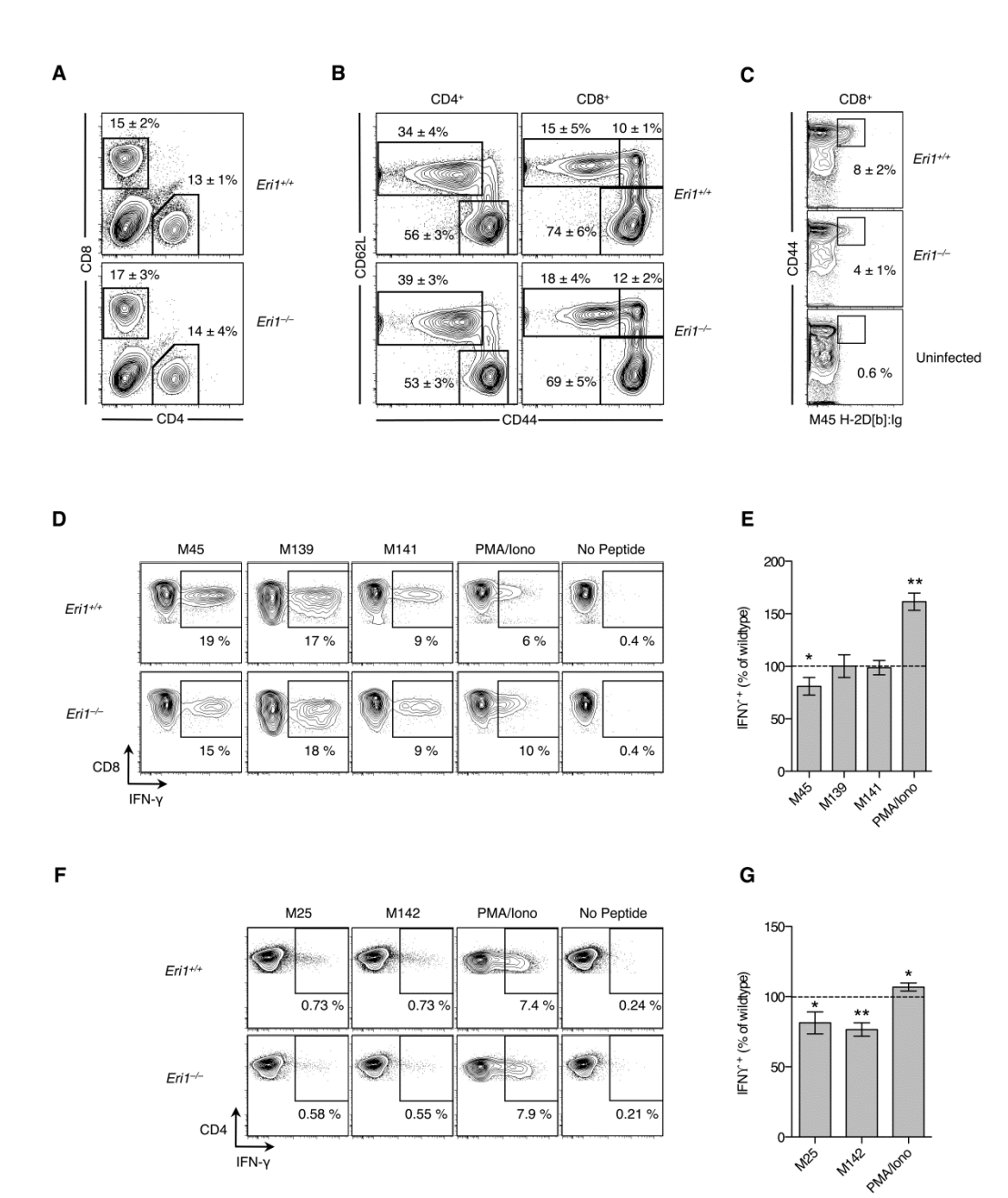


Figure 7

